MURDOCH RESEARCH REPOSITORY

**El-Harbawi, M., Shaaran, S.N.A.Bt.S., Ahmad, F., Wahi, M.A.A.,
Abdul, A., Laird, D.W. and Yin, C-Y (2012)** *Estimating the
flammability of vapours above refinery wastewater laden with
hydrocarbon mixtures.* **Fire Safety Journal, 51 . pp. 61-67.**

http://researchrepository.murdoch.edu.au/8075/

Estimating the flammability of vapours above refinery waste water laden with hydrocarbons mixtures

Mohanad El-Harbawi[1,*], Siti Nurul Asikhin Bt. Shaaran[2], Fatihah Ahmad[1], Muhammad Aizat Abd Wahi[1], Adamu Abdul[3], Damian W. Laird[4], Chun-Yang Yin[4]

[1]*Department of Chemical Engineering, Universiti Teknologi PETRONAS, 31750, Tronoh, Perak, Malaysia*

[2]*Reliability Integrity Engineering, Petronas Carigali Sdn Bhd, Petronas, Jln Belia, 88000 Kota Kinabalu, Sabah, Malaysia*

[3]*Department of Chemical Engineering, Universiti Teknologi Malaysia, 81310, Skudai, Johor-Bahru, Malaysia*

[4]*School of Chemical and Mathematical Sciences, Murdoch University, Murdoch, 6150, Western Australia*

Corresponding author: Tel: +605-3687581, Email: mohanad_elharbawi@petronas.com.my

Abstract

In this study, the likelihood of fire hazards attributed to the vaporization of hydrocarbon components derived from refinery wastewater drainage systems was assessed. Liquid samples containing mixtures of hydrocarbon products and water were collected from a refinery drainage system and subjected to a distillation process to separate oil and water. The oil-liquid phase was analyzed using Gas Chromatography Mass Spectrometry (GC-MS) to examine the composition of the sample. Hydrocarbon compounds ranging from C_9 to C_{16} were detected. Mole fractions of 28 selected components in the liquid phase were obtained from the GC-FID data and used to calculate mole fractions of components in the gas phase via modified Raoult's law. Lower Flammability Limits (*LFL*s) and Upper Flammability Limits (*UFL*s) for individual components were calculated using a stoichiometric concentration method, while the *LFL* and *UFL* values for the mixture (*LFL*$_{mix}$ and *UFL*$_{mix}$) were calculated using the Le Chatelier equation. The *LFL*$_{mix}$ and *UFL*$_{mix}$ values were used to construct a flammability diagram and subsequently used to determine the flammability of the mixture. The findings of this study may assist in minimizing fire hazards associated with presence of hydrocarbon vapours derived from refinery wastewater streams.

Keywords: Gas chromatography; compositions; Lower and Upper Flammability Limits; flammability diagram.

1. Introduction

Refineries are complex systems of numerous chemical process operations that refine crude oil into desired products such as Liquefied Petroleum Gas (LPG), petrochemical naphtha, motor gasoline, kerosene, diesel and other products. Petroleum refineries can consume high quantities of water for operational usage relative to other industrial and domestic users within a geographical region. Consequently, these refineries can generate large volumes of wastewaters containing various petroleum hydrocarbons, heavy metals, sulfur and ammonia at concentrations that typically require treatment (Al-Haddad et al., 2007) prior to final discharge. With respect to hydrocarbon components, highly flammable compounds such as benzene, toluene, ethylbenzene and xylenes may be present and they pose a significant threat of fire hazard. Over time, the mixture of water and hydrocarbon in drainage systems at certain conditions will naturally separate and form distinct liquid phases, based on density and polarity of the material (EPA, 1998). Hydrocarbon compounds from these drainage flows can vary widely in composition from day-to-day due to operational activities such as storage of waste liquids from drains, equipment cleaning and spills. Some of these compounds can evaporate and turn into vapour at ambient temperature and atmospheric pressure, thus creating potentially flammable mixtures in air. The presence of flammable mixtures exposes drainage systems to the possibility of fire and explosion.

The composition of hydrocarbon compounds can be determined and ignitable liquids can be identified (Newman et al, 1997) using comprehensive gas chromatography (GC) systems such as gas chromatography–isotope ratio mass spectrometry (GC–IRMS) and gas chromatography-mass spectrometry (GC-MS). GC analysis can determine the presence, type and concentrations of

70   contaminated hydrocarbons in wastewater (Senn and Johnson, 1987). However, GC analysis of

71   sample compositions is not sufficient to predict the flammability of hydrocarbon mixtures. In this

72   regard, a flammability diagram method can be suitably used for this purpose (Mashuga and

73   Crowl, 1999). Flammability diagrams generally show the "area" of flammability in mixtures of

74   fuel, oxygen and an inert gas. Mixtures of the three gases are usually depicted in a triangular

75   diagram, also known as a Ternary plot. For more detailed information on the ignitability of

76   mixtures and spark ignition, readers are directed to reviews by Mullins (1955), Lewis and von

77   Elbe (1987), and Mullins and Penner (1959).

78   Vapour-air mixtures ignite and burn only over a well-specified range of compositions. The

79   mixture will not burn when the composition is lower than the lower flammable limit (LFL), that

80   is, the mixture is too lean for combustion. The mixture is also not combustible when its

81   composition is too rich, that is, when it is above the upper flammable limit (UFL). As such, a

82   mixture is flammable only when its composition is between LFL and UFL. These flammability

83   limits can be measured experimentally, though they can still be determined without experimental

84   data (Crowl and Louvar, 2002). There are several available methods, databases and software

85   packages that provide sufficient flammability information for various hydrocarbons and they can

86   be sourced from Coward and Jones (1952), Zabetakis (1965), Sax (1984), Kuchta (1985), Ohtani

87   *et al*. (1994), Brooks and Crowl (2007a) and DIPPR (2010).

88   The limiting oxygen concentration (LOC) is defined as the minimum oxygen concentration

89   in a mixture of fuel, air and inert gas that will propagate flame and is expressed in volume

90   percent of oxygen (Zlochower and Green, 2009). In essence, LOC varies with pressure and

91   temperature and depends on the type of inert (non-flammable) gas present. A reaction can not

92   generate enough energy to heat the entire gas mixture required for the self-propagation of the

93 flame if the oxygen concentration is below the LOC (Crowl and Louvar, 2002). As such, the

94 LOC is a useful parameter in terms of fire hazard prevention since explosions and fires can be

95 prevented by reducing the oxygen concentration regardless of fuel concentration. This concept is

96 the basis for a common procedure called *inerting* used in safety engineering (Crowl and Louvar

97 2002; ASTM 2009). The LOC can be measured experimentally using a flammability apparatus

98 (British and European Standard, 2007; ASTM 2008a; ASTM 2008b) or it can be found from

99 different resources (NFPA 1994; CHEMSAFE, 2007). An example of experimental LFL and

100 LOC determination can be found from a study conducted by Brooks and Crowl (2007b), in

101 which they experimentally measured the LFL, LOC and the maximum safe solvent concentration

102 (MSSC) for ethanol and acetonitrile above aqueous solutions. If experimental and/or literature

103 data are not available, the LOC can be estimated using the stoichiometric combustion reaction

104 and the LFL. This procedure works relatively well for many different hydrocarbons (Siwek,

105 1996; Crowl and Louvar, 2002).

106   The objectives of this study were to estimate flammability limits and the LOC of the

107 hydrocarbon vapour mixture above refinery wastewater and subsequently determine the

108 flammability of the mixture. This was achieved by incorporating thermodynamics with process

109 safety concepts. Findings from this study can be used to investigate the root cause of fire

110 incidents in drainage systems due to the presence of flammable hydrocarbon vapour mixtures.

111

112

113

114

115

116 **2.   Methodology**

118 2.1.1 *Liquid Phase*

120   Liquid samples were collected from drainage lines in a refinery located in Malaysia.

121 Residual water was removed from the samples using a simple distillation technique. The

122 composition of the organic-phase liquid was analysed using both GC-MS (for identification) and

123 GC-FID (Flame Ionisation Detection) (for quantitation). GC-MS was performed with a

124 Shimadzu QP5050 GCMS using the following settings: Electron impact ionization, electron

125 energy 70 eV and scan range 40 - 500 amu at 1 scan/s. The carrier gas (Helium 99.999%) flow

126 rate was set to 1.5 ml/min with column inlet pressure 54.8 kPa and linear velocity 36.10 cm/sec.

127 The end of the column was directly introduced into the ion source of a mass selective detector

128 operated in an electron impact ionization mode. Samples were injected into a HP5 fused silica

129 (5% phenyl polysilphenylene-siloxane) capillary column BPX5 (30 m length; 0.25 mm i.d.; 0.25

130 µm film thickness) and the oven temperature was held at 55°C for 2 min. It was then increased to

131 300°C at 5°C/min and thereafter held for 40 minutes. The components of the liquid sample were

132 identified by comparing their mass spectra with the NIST Mass Spectral Database. Pure samples

133 of a selected number of compounds were analysed using the same GCMS conditions in order to

134 verify the match from the database.

135 Quantitative analysis of the peaks was performed with a Shimadzu GC2010 with an FID using

136 the same column and temperature parameters as for the GC-MS analysis.

137 The mass fraction of each component in the liquid phase can be determined from GC-FID data

138 (Eq. 1):

139     $$\chi_i = \frac{A_i}{A_T}$$ (1)

140   where, χ_i is the mass fraction of component i, A_i is the peak area of component i, and A_T is the

141   peak area of all components.

142

143   The mass fraction is converted to mole fraction using Eq. (2):

144     $$x_i = \frac{\chi_i / M_i}{\sum \chi_i / M_i}$$ (2)

145   where, x_i is the mole fraction in liquid phase of component i, and M_i is the molecular weight of

146   component i.

147
148   2.1.2   *Vapour Phase*

149

150   It was necessary to estimate the concentrations of components in the gas phase, which also

151   contributed to the flammability of the mixture. Modified Raoult's law was used to estimate the

152   amount of liquid vaporized at ambient temperature; Eq. (3) was used to calculate the mole

153   fraction in the gas phase.

154     $$\gamma_i \, x_i \, P_i^{sat} = \varphi_i \, y_i \, P_t$$ (3)

155   where γ_i is the activity coefficient for component i, x_i is the mole fraction of in the liquid

156   phase, P_i^{sat} is the vapour pressure of compound i as a pure component, φ_i is the fugacity

157   coefficient for component i, y_i is the mole fraction of component i in the vapour phase, and P_t is

158   the total pressure. Theoretically, the activity coefficient, γ_i, for an ideal solution is equal to 1.

159   However, since the mixture is non-ideal (real), the activity coefficient was calculated using the

7

160 UNIversal Functional Activity Coefficient (UNIFAC) method. The UNIFAC method expresses

161 the activity coefficient as the sum of a combinatorial part, $\ln \gamma_i^C$ and a residual part, $\ln \gamma_i^R$ (Eq.

162 4) (Fredenslund et al., 1975):

163 $$\ln \gamma_i = \ln \gamma_i^C + \ln \gamma_i^R \tag{4}$$

164 $\ln \gamma_i^C$ is given by Eq. (5):

165 $$\ln \gamma_i^C = \ln \frac{\Phi_i}{x_i} + \frac{z}{2} q_i . \ln \frac{\theta_i}{\Phi_i} + l_i + \frac{\Phi_i}{x_i} \sum_{j=1}^{M} x_j l_j \tag{5}$$

166 $$l_j \equiv \frac{z}{2} (r_j - q_j) - (r_j - 1) \tag{6}$$

167 Where z is the average number of nearest neighbours around a group in solution (constant value

168 is used: $z = 10$). The segment fraction, Φ_i, and surface area fraction, θ_i, are defined, respectively

169 by Eqs. (7) and (8):

170 $$\Phi_i = \frac{r_i x_i}{\sum_{j=1}^{M} r_j x_j} \tag{7}$$

171 $$\theta_i = \frac{q_i x_i}{\sum_{k=1}^{M} q_j x_j} \tag{8}$$

172 The molecular volume, r_j, is defined by the sum of its constituent group given by Eq. (9):

173 $$r_j = \sum_{k=1}^{N} v_k^j . R_k \tag{9}$$

174 Where v_k^j is the number of k groups in molecule j, and R_k is the volume of group k. The

175 molecular surface area, q_j, is the sum of the individual group areas in the molecules given by Eq.

176 (10):

177 $$q_j = \sum_{k=1}^{N} v_k^j . Q_k \qquad (10)$$

178 where Q_k is the group surface area.

179 R_k and Q_k are obtained from the van der Waals group volumes and surface areas.

180 $\ln \gamma_i^R$ was calculated from Eq. (11):

181 $$\ln \gamma_i^R = \sum_{k=1}^{N} v_k^i \left[\ln \Gamma_k - \ln \Gamma_k^i \right] \qquad (11)$$

182 where Γ_k^i is the group residual activity coefficient of group k in a reference solution containing

183 only molecules of type i. Γ_k is the group residual activity coefficient in the solution. The

184 coefficients Γ_k^i and Γ_k are related to the composition and temperature according to Eq. (12):

185 $$\ln \Gamma_k = Q_k \left\{ 1 - \ln \left(\sum_{m=1}^{N} \Theta_m . \psi_{mk} \right) - \sum_{m=1}^{N} \left[\frac{\Theta_m . \psi_{km}}{\sum_{n=1}^{N} \Theta_n . \psi_{nm}} \right] \right\} \qquad (12)$$

186 In Eq. (12), the group interaction parameter, ψ_{mk} is defined by Eq. (13):

187 $$\psi_{mk} = e^{-\frac{a_{mk}}{T}}, \quad a_{mk} \neq a_{km} \qquad (13)$$

188 where a_{mk} is the group interaction parameter between groups n and m. The surface contribution,

189 Θ_m and the mole fraction of the group, X_m are defined by Eqs. (14) and (15), respectively:

190 $$\Theta_m \equiv \frac{Q_m . X_m}{\sum_{n=1}^{N} Q_n . X_n} \qquad (14)$$

191 $$X_m \equiv \frac{\sum_{j=1}^{M} v_m^j . x_j}{\sum_{j=1}^{M} \sum_{n=1}^{N} v_n^j . x_j} \qquad (15)$$

9

192 The fugacity coefficient, φ_i, for each component in the mixture was determined using the Peng-

193 Robinson method (Eq. (16) (Peng and Robinson, 1976):

194 $$ln\varphi_i = \frac{b_k}{b}(Z-1) - ln(Z-B) - \frac{A}{2\sqrt{2}B} \times \left(\frac{2\sum_i^N x_i a_{ik}}{a} - \frac{b_k}{b}\right) ln\left(\frac{Z+2.414B}{Z-2.414B}\right) \tag{16}$$

195 where φ_i is the fugacity coefficient, b is van der Waals co-volume defined by Eq. (17), Z is the

196 compressibility factor defined by Eq. (18), B is a constant defined by Eq. (19), A is a constant

197 defined by Eq. (20), x_i is the mole fraction, and a is the attraction parameter defined by Eq.

198 (21):

199 $$b = \sum_i^N x_i b_i \tag{17}$$

200 $$Z = \frac{Pv}{RT} \tag{18}$$

201 $$B = \frac{bP}{RT} \tag{19}$$

202 $$A = \frac{aP}{R^2 T^2} \tag{20}$$

203 $$a = \sum_i^N \sum_j^N x_i x_j a_{ij} \tag{21}$$

204 where P is the pressure defined by Eq. (22), T is the temperature, v is the molar volume, R is the

205 universal gas constant, a_{ij} is defined by Eq. (23), and i, j, k are component identifications.

206 $$P = \frac{RT}{v-b} - \frac{a(T)}{v^2 + 2bv - b^2} \tag{22}$$

207 $$a_{ij} = (1-\delta_{ij})a_i^{1/2} a_j^{1/2} \tag{23}$$

208 where, δ_{ij} is an empirically determined binary interaction coefficient for components i and j.

209 Applying Eq. (24) at the critical point, we obtain:

210 $$a(T_c) = 0.45724 \frac{(RT_c)^2}{P_c} \tag{24}$$

211 $$b(T_c) = 0.07780 \frac{RT_c}{P_c} \tag{25}$$

212 $$Z_c = 0.307$$

213 At temperatures other than the critical:

214 $$a(T) = a(T_c).a(T_r, \omega) \tag{26}$$

215 $$b(T) = b(T_c) \tag{27}$$

216 where $a(T_r, \omega)$ is a dimensionless function of reduced temperature and acentric factor, ω and

217 equals unity at the critical temperature.

218 The total pressure for the mixture can be calculated from Eq. (28):

219 $$P_t = \sum \gamma_i x_i p_i^{sat} \tag{28}$$

220 The vapour pressures of the components were calculated using the classic (Eq. 29) and extended

221 Antoine equations (Eq. 30):

222 $$\log_{10} P^{sat} = A - \frac{B}{C+T} \tag{29}$$

223 $$\log_{10} P^{sat} = A - \frac{B}{T} + C \log_{10} T + DT + ET^2 \tag{30}$$

224 where

225 P^{sat} is the vapour pressure (mmHg) while A, B, C, and D are the component-specific constants.

226 These constants were obtained from several sources (Wichterle and Linek, 1971; Yaws, 1992;

227 Dykyj et al., 1999; Yaws et al., 2009; www.chemspider.com).

11

228   2.2.1   *LFL and UFL*

229   For some situations, it may be necessary to estimate the flammability limits without

230   experimental studies. Jones (1938) found that for many hydrocarbon vapours, the *LFL* and *UFL*

231   were functions of the stoichiometric concentration of fuel (C_{st}) (Eq. 31 and Eq. 32):

232     $LFL = 0.55C_{st}$ (31)

233     $LFL = 3.5C_{st}$ (33)

234   The stoichiometric concentration, C_{st} for organic compounds was determined using the general

235   combustion reaction (Eq. 33).

236     $C_mH_xO_y + zO_2 \rightarrow mCO_2 + \left(\dfrac{x}{2}\right)H_2O$ (33)

237   where z is equivalent moles O_2/moles fuel which can be determined from Eq. (34):

238     $z = m + \dfrac{x}{4} - \dfrac{y}{2}$ (34)

239   The stoichiometric concentration, C_{st} can be determined as a function of z by Eq. (35):

240   C_{st} = [moles fuel/ (moles fuel + moles air)] $\times 100 = \dfrac{100}{[1 + (z/0.21)]}$ (35)

241   Substituting Eq. (34) into Eq. (35) and applying Eq. (31) and Eq. (32) yield Eqs. (36) and (37):

242     $LFL\,(vol\,\%) = \dfrac{0.55(100)}{4.76m + 1.19x - 2.38y + 1}$ (36)

243     $UFL\,(vol\%) = \dfrac{3.50(100)}{4.76m + 1.19x - 2.38y + 1}$ (37)

244   where *LFL* and *UFL* are the lower and upper flammable limits, respectively.

245   The *LFL* and *UFL* for mixtures (LFL_{mix} and UFL_{mix}) were calculated using the Le Chatelier

246   equation (Eqs. 38 and 39) (Le Chatelier, 1891):

247 $$LFL_{mix} (vol\%) = \frac{1}{\sum(y_i/LFL_i)} \qquad (38)$$

248 $$UFL_{mix} (vol\%) = \frac{1}{\sum(y_i/UFL_i)} \qquad (39)$$

249 where LFL_i and UFL_i are the lower and upper flammable limits, respectively, for component i in

250 fuel and air while n represents the number of combustible species.

251

252 2.2.2 *Limiting Oxygen Concentration (LOC)*

253

254   LOC can be estimated using the stoichiometry of the combustion reaction and the *LFL*

255 (Crowl and Louvar, 2002). Eq. (40) can also be used to estimate LOC for a vapour mixture

256 (Zlochower and Green, 2009):

257 $$LOC_{mix} = \sum y_i R_i / \sum y_i / L_i^* = \sum y_i R_i / \sum y_i R_i / LOC_i \qquad (40)$$

258 $$L_i^* = LOC_i / R_i \qquad (41)$$

259 where LOC_{mix} is the limiting oxygen concentration for the vapour mixture (vol%), R_i is the

260 stoichiometric molar ratio of oxygen to compound i in the vapour phase, and LOC_i is the

261 limiting oxygen concentration for individual compound (vol%). Figure 1 shows the methodology

262 outline adopted in this study.

263

264

265

266

267

268   **3.   Results and Discussion**

269

270   3.1   *Compositions*

271

272   The components were identified using a combination of the retention time, comparison of

273   mass spectrum derived from GC-MS analysis of the hydrocarbon mixture to a mass spectral

274   library, and comparison to known standards. Figure 2 shows the retention time and peak

275   abundance data for 77 components detected in the liquid phase via GC-MS analysis. Considering

276   the difficulties of relying solely on mass spectral database matching for the identification of

277   compounds that are very similar in molecular structure, it was felt prudent to take the following

278   precautions in deciding which of the 77 individual compounds observed in the gas

279   chromatogram should be used in calculations. Firstly, using pure compounds that were readily

280   available it was ascertained that peaks 3, 14, 41, 52, 75, and 77 were simple straight chain

281   hydrocarbons (Table S1 - electronic Supplementary material) and that the compound ID from the

282   NIST database matched with the compounds injected. These results confirmed that the output

283   from the mass spectral comparison was valid, particularly for compounds with higher than 95%

284   match. Subsequently, all compounds with a minimum 95% database match were considered to

285   have been correctly identified. As a check on this assumption it was noted that the database

286   identification of peaks 28, 42, 50, and 63 were for simple straight chain alkanes and produced a

287   homologous series with the positively identified compounds. Additionally, it was noted that the

288   difference in retention times between these compounds, running from nonane to hexadecane,

289   were consistent providing further evidence that these were compounds of a homologous

290   hydrocarbon series. There are 28 compounds (Table S1- also contains the properties relevant for

14

291   this study) that meet the above criteria and their order of elution based on their boiling points,

292   (i.e. those with higher boiling points elute later) is also consistent with expected results. These

293   selected 28 compounds cover all the major identified peaks (including numbers 42, 50, 63) and

294   account for a 56% of the total area in the chromatogram (as determined from GC-FID data).

295   The identification of individual components shows that the liquid sample contains a large

296   number of hydrocarbon components ranging from C_9 to C_{16}. The predominant hydrocarbon

297   groups are alkane and alkene with a relatively minor presence of arenes. The peak numbers 14,

298   28, 41, 52, 65, and 75 are assigned to decane, undecane, dodecane, tridecane, tetradecane, and

299   pentadecane, respectively, and these six components constitute more than 43% of the total

300   chromatogram area,. The mass fraction of each component was estimated by dividing the GC-

301   FID peak area of each component by the total peak area. The mass fraction was then converted to

302   mole fraction according to Eq. (2) and the resulting distribution for the mole fraction for each

303   component x_i in the liquid phase is shown in Figure 3.

304

305   3.2   *Mole Fraction in Vapour Phase*

306

307   The activity and fugacity coefficients for all components in the vapour mixture are

308   calculated and the values shown in Table S1. The average activity and fugacity coefficients for

309   the vapour mixture were determined to be 1.02 and 0.88 respectively. Figure 4 shows the mole

310   fraction for each component in the vapour phase, y_i based on combustible basis. Interestingly, the

311   values of y_i for most components are small; possibly due to the low volatility of the heavy

312   hydrocarbon components detected in the liquid phase. The low volatilities of the components

313   were due to the low vapour pressure, which range from 5×10^{-3} mmHg to 6.74 mmHg. The total

314   mole fraction of the vapour mixture is 0.12 vol %, while the air content in the mixture is 99.88

315   vol%. Therefore, the percentages of N_2 and O_2 in the mixture are approximated to be 79 vol%

316   and 21 vol%, respectively.

317

318   3.3   *LFL*, *UFL*, and *LOC*

319

320   The calculated *LFL* and *UFL* as well as *LOC* values are listed in Table S1. The calculated

321   *LFL* and *UFL* values are in agreement with those obtained from other databases and open

322   literatures (Figures 5a and 5b). It should be noted that not all *LFL* and *UFL* values could be

323   found in other database and published literatures and some of these values were not indicated in

324   Table S1. The LFL_{mix} and UFL_{mix} are determined to be 0.72 vol% and 4.60 vol%, respectively

325   while the LOC_{mix} value is 11.40 vol%.

326

327   3.4   *Flammability Diagram*

328

329   A flammability diagram is a conventional method used to assess the flammability of mixture

330   of gases. The flammability diagram is represented by three axes, namely, (1) fuel (hydrocarbon

331   vapour mixture), (2) inert material, and (3) oxygen. In order to plot the flammability diagram,

332   concentrations of the fuel, oxygen, and inert material (in volume or mole %) are required. The air

333   line is plotted by taking the compositions of air from Table S1 (78.91 % nitrogen and 20.98 %

334   oxygen). The intersection of the stoichiometric line with the oxygen axis is given by $100(z/1+z)$

335   (Crowl and Louvar, 2002). The LOC_{mix} line can be drawn by locating the LOC_{mix} value (11.40%)

336   on the air axis and then drawing a parallel line until it intersects with the stoichiometric line. To

337   construct the flammability zone, the values of LFL_{mix} and UFL_{mix} are required and they are

338   located on the air line while the flammability zone is the area to the right of the air line. Figure 6

339   represents the triangular flammability diagram for the hydrocarbon mixture. It can be clearly

340   seen that the stoichiometric line crosses the flammable zone. Therefore, it can be inferred that the

341   vapour mixture is flammable.

342

343   **4.   Conclusions**

344

345   In this study, theoretical work including thermodynamic fundamentals and flammability

346   calculations were applied to estimate the flammability limits of hydrocarbon vapours derived

347   from refinery wastewater. Detailed inspection of the customised flammability diagram showed

348   that the vapour mixture derived from the wastewater was flammable and may pose a potential

349   fire hazard. As such, it is always prudent for refinery workers to exercise caution when handling

350   wastewater laden with hydrocarbon residuals. Findings from this study afford a useful basis for

351   safety officers and engineers from other refineries to assess the potential fire hazards associated

352   with hydrocarbon vapours derived from wastewater streams.

353

354   **References**

355

356   Al-Haddad A., Chmielewská E., and Al-Radwan S., (2007). A Brief Comparable Lab

357   Examination for Oil Refinery Wastewater Treatment using the Zeolitic and Cabonaceous

358   Adsorbents. *Petroleum & Coal* 49 (1): 21-26.

359

360   ASTM (2008a). Standard test method for concentration limits of flammability

361   of chemicals (vapors and gases). E681-04. In: ASTM International annual book of standards,

362   Vol. 14.02. West Conshohocken, PA: American Society for Testing and Materials.

363

364   ASTM (2008b). Standard test methods for limiting oxygen (oxidant) concentration in gases and

365   vapors. E2079-07. In: ASTM International annual book of standards, Vol. 14.02. West

366   Conshohocken, PA: American Society for Testing and Materials.

367

368   ASTM (2009). Standard Test Method for Measuring the Minimum Oxygen Concentration to

369   Support Candle-Like Combustion of Plastics (Oxygen Index). D2863-09. *American Society for*

370   *Testing and Materials (ASTM).*

371

372   British and European Standard. (2007). Determination of limiting oxygen concentrations of

373   gases and vapours. EN 14756. rue de Stassart, 36, B-1050 Brussels, Belgium: CEN European

374   Committee for Standardization.

375

376   Brooks, M., Crowl, D., (2007a). Flammability Envelopes for Methanol, Ethanol, Acetonitrile and

377   Toluene. *Journal of Loss Prevention in the Process Industries* 20: 144–150.

378

379   Brooks, M., Crowl, D., (2007b). Vapor Flammability above Aqueous Solutions of Flammable

380   Liquids. *Journal of Loss Prevention in the Process Industries* 20: 477–485.

381

382   CHEMSAFE, (2007). Database of evaluated safety characteristics. Frankfort/M, Germany:

383   DECHEMA, BAM, and PTB.

384

385   ChemSpider (Database of Chemical Structures and Property Predict.

386   www.chemspider.com

387

388   Coward, H. F. and Jones, G. W., (1952). Limits of Flammability of Gases and Vapors. *Bulletin*

389   *503, Bureau of Mines*.

390

391   Crowl D., A, Louvar J. F., (2002). Chemical Process Safety: fundamentals with applications.

392   *Prentice-Hall*.

393

394   DIPPR, (2010). DIPPR® Project 801. Evaluated Standard Thermophysical Property Values.

395   American Institute of Chemical Engineers Design Institute for Physical Properties.

396

397   Dykyj J., Svoboda J., Wilhoit R., Frenkel M., Hall K., (1999). Vapor Pressure of Chemicals.

398   *Springer*, Vol. 20.

399

400   EPA, (1998). EPA Chemical Accident Investigation Report. *United States Environmental*

401   *Protection Agency*.

402

403   Fredenslund, A. Jones, R. L. Prausnitz, J. M., (1975). Group-Contribution Estimation of Activity

404   Coefficients in Nonideal Liquid Mixtures. *AIChE J.* 21: 1086–1099.

405   Jones, G. W., (1938). Inflammation Limits and their Practical Application in Hazardous

406   Industrial Operations. *Chemical Review*s, 22 (1): 1-26.

407

408   Kuchta, J. M., (1985). Investigation of Fire and Explosion Accidents in the Chemical, Mining,

409   and Fuel-related Industries-A manual. *Bureau of Mines Bulletin*, *680*.

410

411   Le Chatelier H., (1891). Estimation of Firedamp by Flammability Limits. *Ann. Mines*, ser. 8, 19:

412   388-395.

413

414   Lewis, B., von Elbe, G., (1987). Combustion Flames and Explosions of Gases. *Academic Press*,

415   pp 731.

416

417   Mashuga, C. and Crowl D., (1999). Flammability Zone Prediction Using Calculated Adiabatic

418   Flame Temperatures. Process Safety Progress, 18 (3): 127-134,

419

420   Mullins, B. P, (1955). Spontaneous Ignition of Liquid Fuels. *Butterworths Scientific*

421   *Publications*, London, pp. 117.

422   Mullins B. P., and Penner, S. S., (1959). Explosions, Detonation, Flammability and Ignition.

423   *Pergamon Press, Inc*., New York, pp. 199.

424

425   Newman R., Gilbert, M., Lothridge, K., (1997). GC-MS Guide to Ignitable Liquids. CRC-Press.

426

427   NFPA 68, Venting of Deflagrations (Quincy, MA: National Fire Protection Association, 1994).

428 Ohtani, H., Lee, S. G., and Uehara, Y., (1994). Combustion Characteristics of Several

429 Flammable Gases with Chlorine Trifluoride. *Proceedings of the Fourth International Symposium*

430 *on Fire Safety Science, Ottawa, Canada.*

431

432 Peng, D. Y., and Robinson, D. B. (1976). A New Two-Constant Equation of State. *Ind. Eng.*

433 *Chem. Fundam.,* 15 (1): 59-64.

434

435 Sax, N. I., (1984). Dangerous Properties of Industrial Materials. *New York: Van Nostrand*

436 *Reinhold Co.*

437

438 Senn, R., and Johnson, M., (1987). Interpretation of Gas Chromatographic Data in Subsurface

439 Hydrocarbon Investigations. *Ground Water Monitoring & Remediation*, 7(1): 58–63.

440

441 Siwek, R., (1996). Determination of Technical Safety Indices and Factors Influencing Hazard

442 Evaluation of Dusts. *Journal of Loss Prevention in the Process Industries*, 9(1): 21-31.

443

444 Wichterle, I., Linek, J., (1971). Antoine vapor pressure constants of pure compounds. *Academia,*

445 *Prague.*

446

447 Yaws, C. L., Narasimhan, P. K., Gabbula Chaitanya, (2009). Yaws' Handbook of Antoine

448 Coefficients for Vapor Pressure. *Knovel library.*

449

450   Yaws, C. L., (1992). Handbook of Thermodynamic Diagrams, Organic Compound C_8 to C_{28},

451   Vol. 3 (Library of Physico-Chemical Property Data). *Gulf Professional Publishing*.

452

453   Zabetakis, M. G. (1965). Flammability Characteristics of Combustible Gases and Vapors.

454   *Bulletin 627, Bureau of Mines*.

455

456   Zlochower, I., Green, G., (2009). The Limiting Oxygen Concentration and Flammability Limits

457   of Gases and Gas mixtures. *Journal of Loss Prevention in the Process Industries* 22: 499-505.

458

459

460

461

462

463

464

465

466

467

468

469

470

471

472

473   **Figure Captions**

474

475   **Fig.1.** Flowchart on the methodology used in this study.

476   **Fig. 2**. GC analysis for the liquid sample.

477   **Fig. 3**. Percentages of hydrocarbon mole fractions in the liquid phase.

478   **Fig. 4**. Percentages of hydrocarbon mole fractions in the vapour phase.

479   **Fig. 5a&b.** Comparison between calculated and literature values of *LFL and UFL*.

480   **Fig. 6**. Triangular flammability diagram of the hydrocarbon mixture.

481

482

483

484

485

486

487

488

489

490

491

492

493

494

495

496

497

498

499

500

501

502

503

504

505

506

507

508

509

510

511

512

513

514
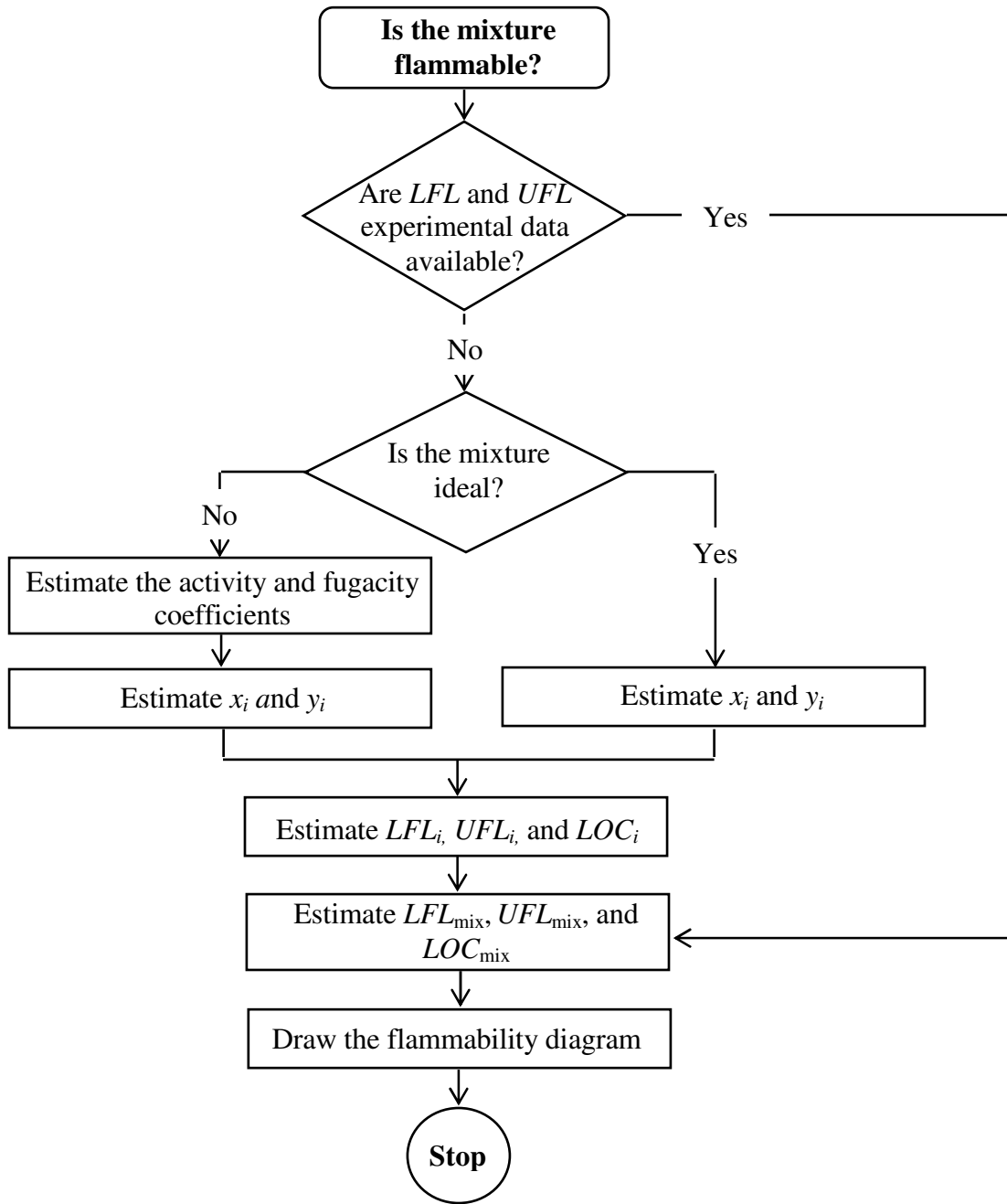
515   **Fig. 1**: Flowchart on the methodology used in this study.

516

517

518

519
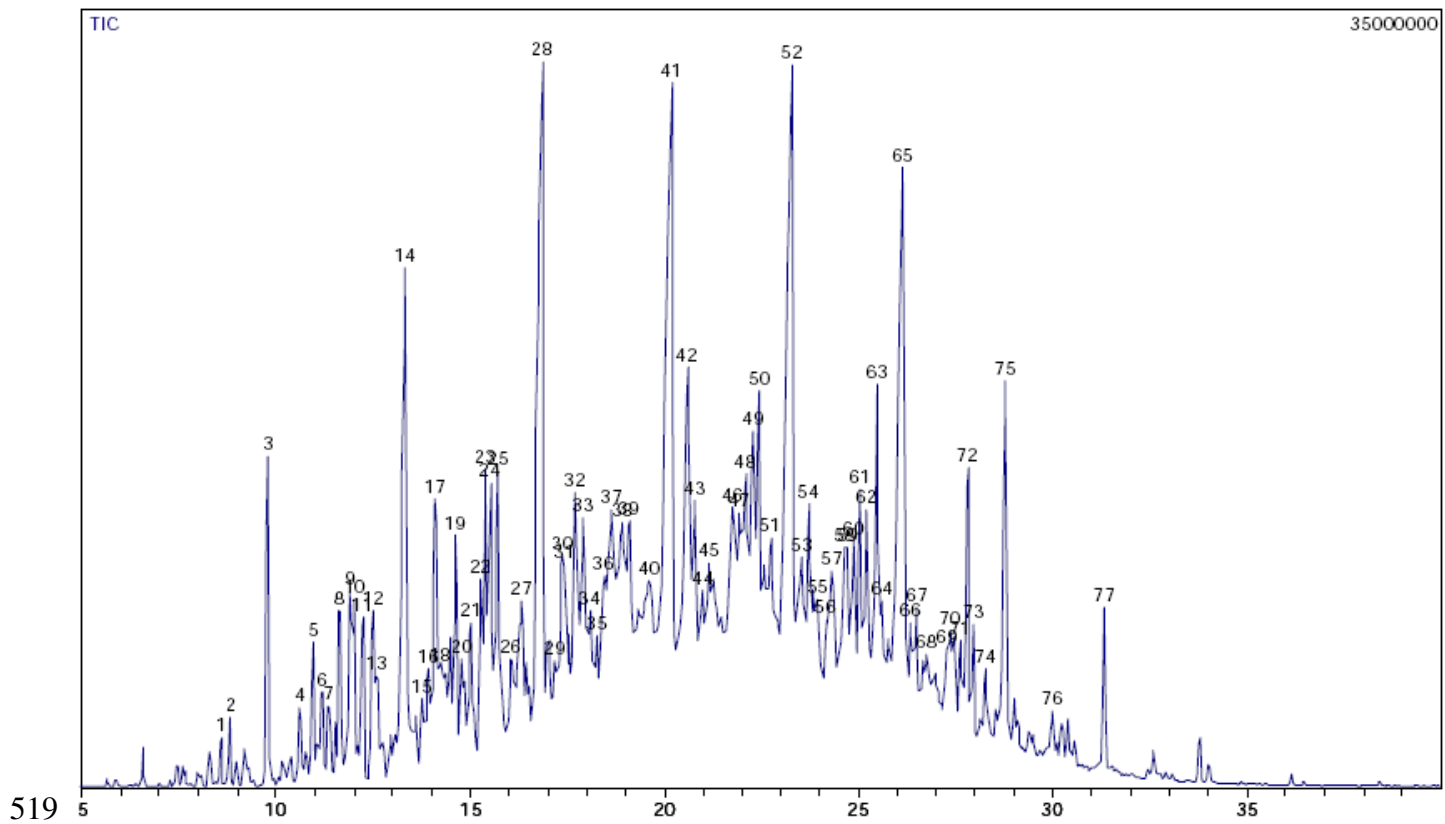
Fig. 2. GC-MS analysis for the liquid sample.

520
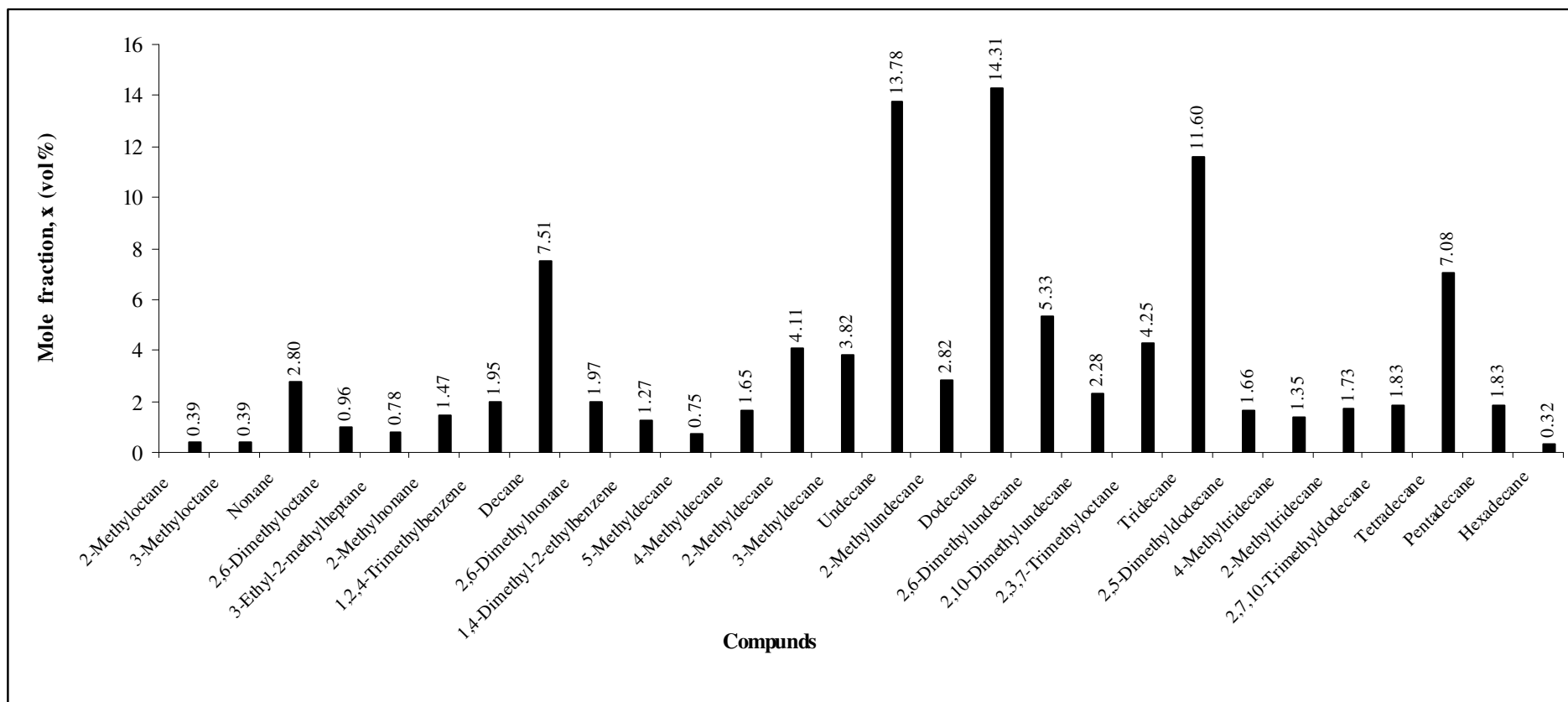
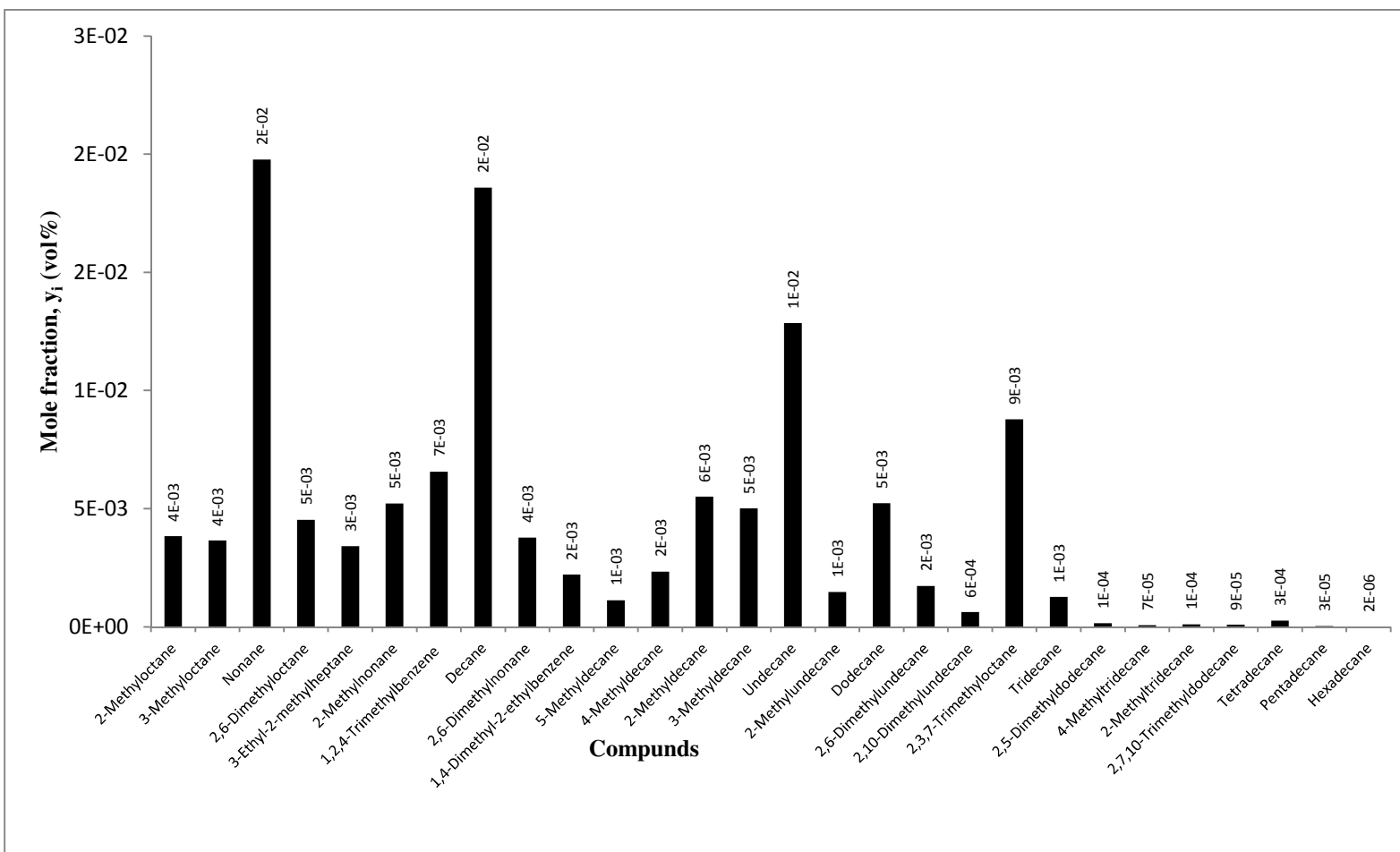**Fig. 3**. Mole fractions of the selected 28 hydrocarbon components in the liquid phase.

Fig. 4. Mole fractions of the selected 28 hydrocarbon components in the vapour phase.
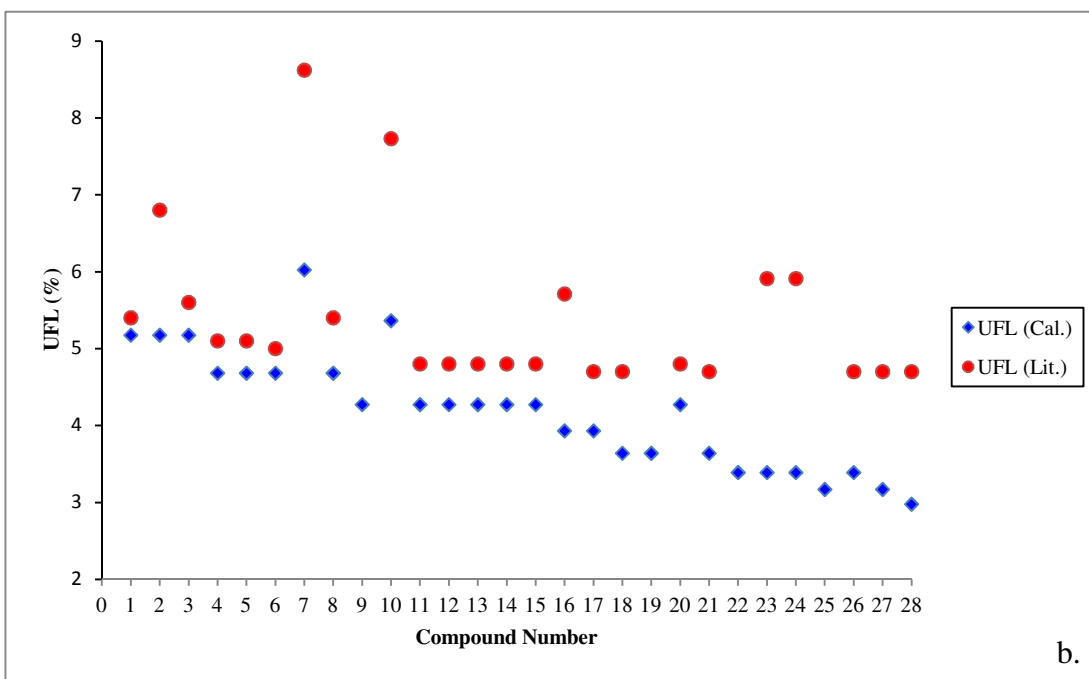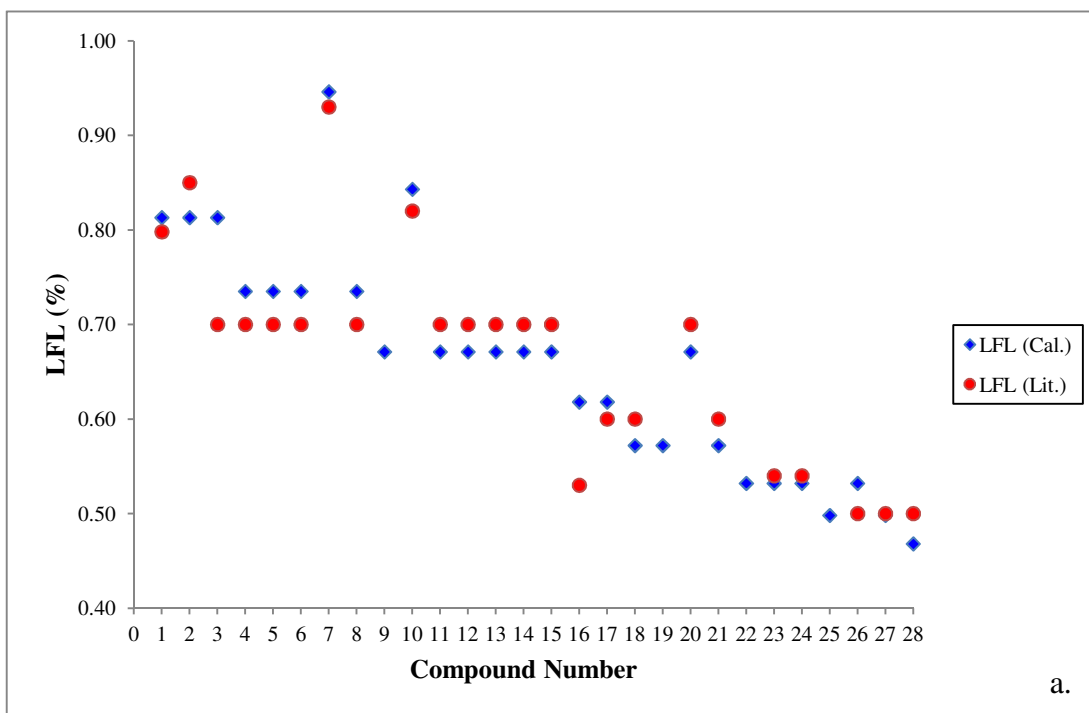
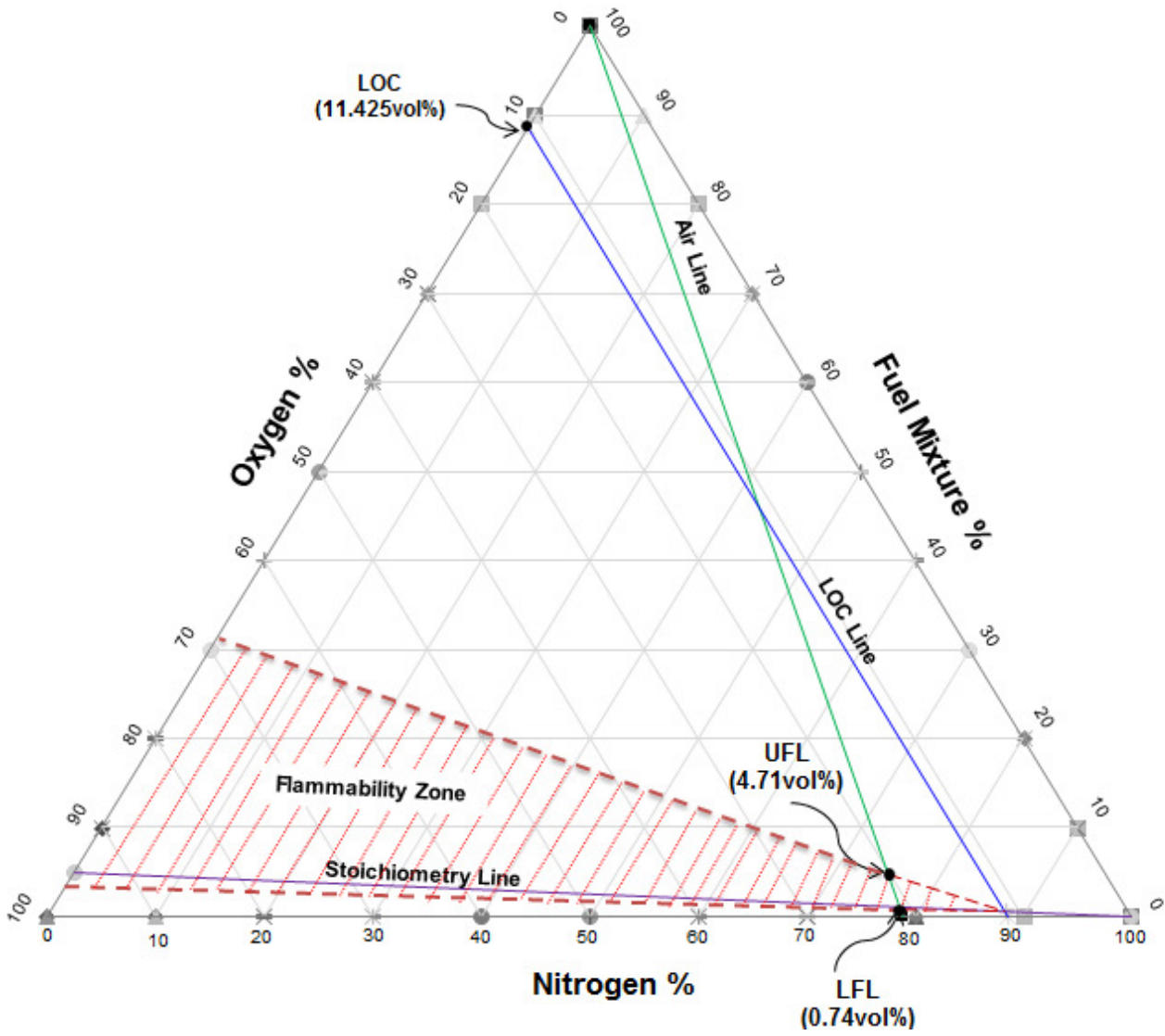`**Fig. 5a &b**. Comparison between calculated and literature values of *LFL* and *UFL*.

Fig. 6. Triangular flammability diagram of the hydrocarbon mixture.